(Received 13 February 2026, Accepted 27 March 2026, Scheduled 14 April 2026)

Efficient Reconfigurable Synthesis of Sparse Arrays with Minimum Spacing Constraints via Group Off-Grid Orthogonal Matching Pursuit

Kunyu Gao[1,*], Yong Lv[1], Zixuan Wang[2], and Mingwei Shen[2]

[1] College of Information Science and Engineering, Hohai University, Changzhou, China
[2] College of Computer Science and Software Engineering, Hohai University, Nanjing, China

ABSTRACT: To reduce the implementation complexity of reconfigurable sparse arrays, this study proposes a low-complexity group-sparse orthogonal matching pursuit (G-OMP) algorithm with a minimum spacing constraint for synthesizing of sparse arrays with multiple beam-shared element positions. An off-grid OMP algorithm with a minimum spacing constraint can mitigate the accuracy degradation caused by fixed-grid discretization, thereby ensuring the practical feasibility of engineering implementations. To enable beam reconfigurability, a group-sparse structure is incorporated into the off-grid OMP algorithm, and a multi-beam group-sparse reconstruction algorithm based on a dynamic grouping strategy is proposed, allowing multiple beams to share sparse array element positions. Simulation results show that, under the simulation parameters, the proposed algorithm achieves low computational complexity while maintaining good radiation pattern performance.

1. INTRODUCTION

With the rapid development of radar, sonar, and wireless communication systems, multi-beam array antenna systems play an increasingly important role in enhancing spatial resolution and enabling efficient signal processing [1]. Sparse arrays have emerged as effective array optimization techniques, capable of maintaining radiation pattern performance while significantly reducing the number of array elements, thereby lowering system hardware costs [2]. In particular, for multi-beam applications, reconfigurable sparse array designs allow the array to flexibly adjust its radiation patterns according to different mission requirements, thereby enabling coordinated multi-beam coverage. With the continued development of multifunction radar and sixth-generation integrated sensing, array antennas are required not only to generate high-gain directive beams, but also to rapidly switch among and realize multiple radiation patterns on a common hardware platform [3]. Compared with deploying separate arrays for different tasks, reconfigurable arrays can achieve multi-beam radiation through aperture sharing, thereby offering clear advantages in reducing hardware scale and improving operational flexibility [4, 5]. However, most existing sparse array design methods focus on optimizing a single radiation pattern, which makes it difficult to satisfy the requirement that multiple radiation patterns share a common set of array element positions. Therefore, achieving satisfactory array synthesis performance while simultaneously considering computational complexity and the minimum spacing constraint required for practical engineering implementation has become a challenging problem in the design of multi-beam reconfigurable sparse arrays.

Research on multi-beam sparse array synthesis can be generally categorized into global optimization [6], matrix pencil, and conventional compressive sensing methods. Global optimization methods formulate sparse array synthesis as a high-dimensional binary optimization problem and typically employ intelligent optimization algorithms, such as particle swarm optimization and genetic algorithms [7, 8]. For large-scale arrays, these methods require global searches over high-dimensional combinatorial spaces and usually rely on multiple random initializations to avoid local optima, resulting in exponentially increasing computational complexity, which makes them unsuitable for large-array design. Wang et al. [9] proposed a unitary matrix pencil method, in which Hankel block matrices are constructed from multi-beam sampled data, and array element positions and excitation parameters are directly estimated through eigenvalue decomposition of the equivalent matrix pencil. Although this method avoids complicated nonlinear optimization, the matrix dimension grows rapidly with an increasing number of sampling points, leading to a significant increase in computational complexity. In recent years, compressive sensing-based sparse array synthesis methods have been extensively studied in the field of array signal processing. Since the introduction of autocorrelation-based theory, remarkable progress has been achieved in sparse array design [10]. Bayesian compressive sensing performs sparse reconstruction via maximizing a posteriori estimation [11]. However, to achieve satisfactory radiation pattern synthesis performance, a dense set of candidate array elements is usually required in the initial stage, which may result in excessively small spacing in the sparse solution and consequently strong mutual coupling effects in practical systems [12]. To address this issue, Wang et al. proposed an iter-

* Corresponding author: Kunyu Gao (13222562050@163.com).

ative sparse reconstruction method based on non-convex optimization [13], which combines a multiple measurement vector model with collaborative sparse reconstruction to enable multiple beams to share a common sparse array structure. After fixing the excitation coefficients, a row-energy-based sliding window constrained optimization strategy is introduced, ensuring that at most, one array element is retained within any consecutive grid interval, thereby indirectly satisfying the minimum spacing constraint. However, this non-convex approach relies on iterative reweighting and repeated matrix updates, which results in a relatively high computational burden in large-scale array design. In addition, although such a sparsification strategy may achieve a slightly smaller number of active elements under the same aperture and minimum spacing constraints, its computational cost increases significantly with the array size.

In summary, existing multi-beam reconfigurable sparse array design methods have difficulty in simultaneously satisfying the requirements of synthesis accuracy, computational complexity, and minimum spacing constraints. Therefore, in this study, we propose a low-complexity group-sparse orthogonal matching pursuit algorithm (G-OMP) for reconfigurable sparse array synthesis, in which multiple radiation patterns share a common set of array element positions. The proposed algorithm adaptively performs dynamic group assignment and reconstruction based on the correlation between the current residual and dictionary atoms, thereby avoiding cross-group redundancy caused by conventional fixed grouping strategies. Moreover, within the off-grid OMP framework, a projected gradient method is employed to enforce the minimum spacing constraint, thereby effectively suppressing mutual coupling effects between adjacent array elements.

2. OFF-GRID OMP WITH MINIMUM SPACING CONSTRAINT

Assume that signals impinge from different directions θ_p $(p = 1, 2, \ldots, P)$ onto a uniform linear array consisting of M elements, where the spacing is half a wavelength. Let $\{x_m\}_{m=1}^{M}$ denote the positions of the array elements along the array coordinate axis. Then, the array steering matrix can be expressed as

$$\begin{aligned}\mathbf{A} &= \begin{bmatrix} e^{\mathrm{j}\frac{2\pi}{\lambda}x_1\sin\theta_1} & \cdots & e^{\mathrm{j}\frac{2\pi}{\lambda}x_M\sin\theta_1} \\ \vdots & \ddots & \vdots \\ e^{\mathrm{j}\frac{2\pi}{\lambda}x_1\sin\theta_P} & \cdots & e^{\mathrm{j}\frac{2\pi}{\lambda}x_M\sin\theta_P} \end{bmatrix} \\ &= [\mathbf{a}(x_1), \mathbf{a}(x_2), \ldots, \mathbf{a}(x_M)]. \end{aligned} \tag{1}$$

where λ denotes the wavelength of the received signal; $\theta_p \in [-90°, 90°]$ represents the observation angle of the radiation pattern; and $\mathbf{a}(x_m)$ represents the array steering vector.

The array radiation pattern at an arbitrary angle θ can be expressed as

$$S(\theta) = \sum_{m=1}^{M} w_m e^{\mathrm{j}\frac{2\pi}{\lambda}x_m\sin\theta} \tag{2}$$

It can be reformulated into a matrix equation as

$$\mathbf{S} = \mathbf{A}\mathbf{w} \tag{3}$$

where w_m denotes the excitation weight of the m-th array element, and $\mathbf{w} = [w_1, w_2, \ldots, w_M]^{\mathsf{T}}$.

Let $\mathbf{S}_d$ denote the desired radiation pattern. According to compressive sensing theory, the sparse synthesis problem of a one-dimensional linear array can be formulated as follows:

$$\arg\min_{\mathbf{w}} \|\mathbf{w}\|_0 \quad \text{s.t.} \quad \|\mathbf{S}_d - \mathbf{A}\mathbf{w}\|_2^2 \le \varepsilon \tag{4}$$

where $\|\mathbf{w}\|_0$ denotes the ℓ_0-norm of the weight vector $\mathbf{w}$, and ε is a predefined tolerance threshold.

The OMP algorithm operates iteratively by selecting, at each iteration, the atom that best matches the desired signal and incorporating it into the reconstructed signal. Specifically, at the t-th iteration, the atom that is most correlated with the current residual is selected based on the projection of the residual onto the steering matrix:

$$\arg\max_{p} |[\mathbf{z}_t]_p| = \arg\max_{p} \left|[\mathbf{A}^{\mathsf{H}}\mathbf{r}_t]_p\right|. \tag{5}$$

where $\mathbf{r}_t$ denotes the current residual, and $\mathbf{z}_t$ is the projection vector. The p-th element of $\mathbf{z}_t$ is denoted by $[\mathbf{z}_t]_p$, and p_t represents the index of the selected column corresponding to the p-th column of the steering matrix $\mathbf{A}$ at the t-th iteration.

The selected column indexed by p_t is grouped to form a matrix and added to the support set. Subsequently, the weight vector w is updated by performing least-squares estimation in the subspace spanned by the selected atoms:

$$\mathbf{w}_{t+1} = \min_{\mathbf{f}:\mathrm{supp}(\mathbf{f})\subseteq\Lambda_{t+1}} \|\mathbf{S}_d - \mathbf{A}\mathbf{f}\|_2^2. \tag{6}$$

where $\mathbf{f}$ denotes the sparse vector.

Insufficient grid discretization may degrade the accuracy of the estimated array element positions, whereas an overly dense grid not only increases the computational complexity but may also lead to a larger number of nonzero elements in the solution. To address this issue, Yang et al. proposed an off-grid compressive sensing-based approach [14]. After t array elements have been selected by the standard OMP algorithm, both the element positions x_k and the excitation weights w_k are further refined, while ensuring that the minimum spacing constraint between adjacent elements is satisfied. The steering vector of each selected array element with respect to its position is approximated by Taylor expansion as follows:

$$\mathbf{a}(x_k + \eta_k x_k) \approx \mathbf{a}(x_k) + \eta_k x_k \frac{\partial \mathbf{a}(x_k)}{\partial x_k} \tag{7}$$

where η_k denotes the perturbation coefficient for the k-th array element.

According to the Taylor series expansion, the aforementioned sparse synthesis problem can be therefore reformulated as follows:

$$\min_{\{\eta_k\}} \left\| \mathbf{r} - \sum_{k=1}^{t} w_k \eta_k x_k \frac{\partial \mathbf{a}(x_k)}{\partial x_k} \right\|_2^2$$

$$\mathbf{r} = \mathbf{S}_d - \sum_{k=1}^{t} w_k \mathbf{a}(x_k) \tag{8}$$

$$-\frac{x_k - x_{k-1}}{2} < \eta_k x_k < \frac{x_{k+1} - x_k}{2}$$

Based on the i-th iteration, the partial derivative matrix is constructed as follows:

$$\mathbf{P}_i = \left[w_1 x_1 \frac{\partial \mathbf{a}(x_1)}{\partial x_1}, w_2 x_2 \frac{\partial \mathbf{a}(x_2)}{\partial x_2}, \ldots, w_t x_t \frac{\partial \mathbf{a}(x_t)}{\partial x_t} \right] \quad (9)$$

Consequently, the optimization of η_k can be reformulated as a constrained least-squares problem, in which the update direction is obtained via the pseudo-inverse matrix, and the constraints are enforced through a projection operation. The update of the k-th selected element position is given by

$$x_k^{i+1} = \max\left\{ x_{k-1}^i + D, \min\left\{ x_{k+1}^i - D, x_k^i + k\, x_k^i \Re\left((\mathbf{P}_i^{\dagger} \mathbf{r}_i)_k \right) \right\} \right\}. \quad (10)$$

where $\Re(\cdot)$ denotes the real part; k is the learning rate; and $\mathbf{P}_i^{\dagger} = (\mathbf{P}_i^{\mathsf{H}} \mathbf{P}_i)^{-1} \mathbf{P}_i^{\mathsf{H}}$ corresponds to the steepest descent direction in the least-squares sense. The residual is set to $\mathbf{r}_t^i = \mathbf{S}_d - \sum_{k=1}^{t} w_k \mathbf{a}(x_k)$.

3. GROUP-SPARSE OMP ALGORITHM WITH MINIMUM SPACING CONSTRAINTS

Although the aforementioned off-grid OMP algorithm with minimum spacing constraints achieves satisfactory off-grid correction capability and sidelobe-suppression performance in single-beam sparse array synthesis, practical engineering applications often require the simultaneous formation of multiple independent beams with different pointing directions. If the conventional beam-by-beam independent design strategy is adopted, each beam will activate a distinct set of array element positions, resulting in a significant increase in the total number of array elements and consequently a substantial rise in hardware cost. Therefore, group-sparse optimization is introduced to enable multiple beams to share a common set of array element positions while preserving multi-beam performance. However, conventional GOMP algorithms rely on fixed group partitioning, which tends to select redundant atoms when crossing group boundaries. To overcome this limitation, a greedy algorithm is proposed that does not require predefined grouping, but instead dynamically expands the group around the peak of the current residual. Consider a uniform linear array with an aperture length of $D = (M-1)\Delta d$. All beams share the same set of array element positions x_m, while each beam is associated with its own excitation vector $\mathbf{w}^l$. The radiation pattern of the l-th beam at angle θ can be expressed as

$$S^l(\theta) = \sum_{m=1}^{M} w_m^l \, e^{\mathrm{j}\frac{2\pi}{\lambda} x_m \sin\theta} \quad (11)$$

where w_m^l denotes the excitation coefficient of the m-th array element for the l-th radiation pattern.

At the angular sampling points θ_p $(p = 1, 2, \ldots, P)$, the l-th radiation pattern can be expressed in vector form as

$$\mathbf{S}^l = \left[S^l(\theta_1), S^l(\theta_2), \ldots, S^l(\theta_P) \right]^{\mathsf{T}} \quad (12)$$

For each desired radiation pattern $\mathbf{S}_d^l$, a sparse weight vector $\mathbf{w}^l$ is determined such that a linear combination of a small number of columns from the observation matrix can closely approximate the desired pattern. In the compressive sensing framework, group sparsity is integrated with the off-grid OMP algorithm, and the multi-beam sparse array synthesis problem can be formulated as

$$\begin{aligned} &\min \|\mathbf{w}^l\|_0 \ \text{ s.t. } \left\| \mathbf{S}_d^l - \mathbf{A}\mathbf{w}^l \right\|_2^2 \\ &= \left\| \mathbf{S}_d^l - \sum_{k=1}^{t} w_k^l \, \mathbf{a}(x_k + \eta_k x_k) \right\|_2^2 \le \varepsilon \\ &-\frac{x_k - x_{k-1}}{2} < \eta_k x_k < \frac{x_{k+1} - x_k}{2} \end{aligned} \quad (13)$$

where $\mathbf{S}_d^l = [S_d^l(\theta_1),\, S_d^l(\theta_2),\, \ldots,\, S_d^{(l)}(\theta_P)]^{\mathsf{T}}$ denotes the observation vector of the l-th desired radiation pattern sampled at P angular points.

In multi-beam radiation pattern reconstruction, the residual matrix at the i-th iteration is given by

$$\begin{aligned} \mathbf{R}^{i-1} &= \left[\mathbf{r}_1^{i-1}, \mathbf{r}_2^{i-1}, \ldots, \mathbf{r}_L^{i-1} \right] \\ \mathbf{r}_l^{i-1} &= \mathbf{S}_d^l - \mathbf{S}^l \end{aligned} \quad (14)$$

The multi-beam synthesis correlation with respect to the j-th dictionary column $\mathbf{a}_j$ is computed as

$$p_j = \sqrt{\sum_{l=1}^{L} \left| \mathbf{a}_j^{\mathsf{H}} \mathbf{r}_l^{i-1} \right|^2} \quad (15)$$

After excluding the previously selected support set and memory set, the column having the maximum correlation was chosen as the center. At this stage, the current window radius was set to $n = 0$, and the optimal group $\mathcal{G}$ was initialized as an empty set.

$$\arg\max_j \ p_j \quad (16)$$

The dynamic group assignment reconstruction algorithm assumes that the two columns adjacent to the center are nonzero. After identifying the center, a local group is dynamically expanded on both sides of the center, and the left and right neighboring columns are added to the support set:

$$\mathcal{G}^i = \left\{ j^i - n,\ j^i,\ j^i + n \right\}, \quad n = 1 \quad (17)$$

During the expansion process, least-squares estimation is performed for each beam l over the current temporary support set to update the excitation coefficients and residuals:

$$\mathbf{w}_i^l = \left(\left(A_{\Lambda^i}^l \right)^H A_{\Lambda^i}^l \right)^{-1} \left(A_{\Lambda^i}^l \right)^H S_d^l \quad (18)$$

$$\mathbf{r}_i^l = S_d^l - A_{\Lambda^i}^l \mathbf{w}_i^l \quad (19)$$

where $\Lambda^i = \Lambda^{i-1} \cup G^i$ denotes the current support set.

By comparing $\mathbf{r}_i^l$ and $\mathbf{r}_{i-1}^l$,

$$\left\| \mathbf{r}_i^l \right\|_2 - \left\| \mathbf{r}_{i-1}^l \right\|_2 \le THR \quad (20)$$

If the correct column is selected, the residual decreases significantly. In this case, the expansion toward both sides continues, and the temporary support set is updated accordingly:

$$\mathcal{G}^{i+1} = \{j^i - 2n,\ j^i - n,\ j^i,\ j^i + n,\ j^i + 2n\} \tag{21}$$

At this stage, least-squares estimation is performed using the four columns surrounding the center to update the excitation coefficients and residuals. However, if an incorrect column is selected, the residual does not exhibit a noticeable improvement, and the algorithm enters a pruning stage. Because the peak is located at the center of the group, the pruning process reduces the number of selected columns in the current iteration by half, and the window radius is updated as $n = n/2$, while retaining the columns closer to the center. If no improvement is observed when $n = 0$, the expansion process is terminated, and the index corresponding to the failed expansion side is recorded in a memory table to avoid redundant computations. Finally, an off-grid position refinement is performed on the final support set, followed by a least-squares update of the excitation coefficients and residuals.

According to the optimization criterion:

$$\left\| \mathbf{S}_d^{(l)} - \sum_{k=1}^{t} w_k^{(l)}\, \mathbf{a}(x_k + \eta_k x_k) \right\|_2^2 \le \varepsilon \tag{22}$$

The iteration is terminated when the deviation between the reconstructed and desired radiation patterns falls below a predefined tolerance threshold. In summary, the whole synthesis flow is illustrated in Algorithm 1.

Algorithm 1. G-OMP with Minimum Spacing Constraint

Input: Desired multi-beam patterns $\mathbf{S}_d^l$, steering matrix $\mathbf{A}$, minimum spacing D, learning rate κ, pruning threshold THR, and tolerance ε.
Output: Element positions $\{x_m\}$ and excitation coefficients $\{\mathbf{w}^l\}$.

Initialize: Residual $\mathbf{R}^0 = \mathbf{S}_d^l$, solution support $\Lambda^0 = \varnothing$, and memory table $\mathcal{V}^0 = \varnothing$.
Iteration
Maximum correlation index

$$j^i = \arg \max_{j \notin \Lambda^i \cup \mathcal{V}^i} p_j^i, \quad p_j^i = \sqrt{\sum_{l=1}^{L} \left| \mathbf{a}_j^H \mathbf{r}_l^{i-1} \right|^2}, \quad j = 1, \ldots, N$$

Update the temporary support

$$G^i = \{j^i - n,\ j^i,\ j^i + n\}, \quad n = 1, \quad \Lambda^i = \Lambda^{i-1} \cup G^i$$

Update the excitation coefficients and residual

$$\mathbf{W}_i = \left((\mathbf{A}_{\Lambda^i})^H \mathbf{A}_{\Lambda^i} \right)^{-1} (\mathbf{A}_{\Lambda^i})^H \mathbf{S}_d^l, \quad \mathbf{R}_i = \mathbf{S}_d^l - \mathbf{A}_{\Lambda^i} \mathbf{W}_i$$

If $\|\mathbf{R}^i\|_2 - \|\mathbf{R}^{i-1}\|_2 < THR$
  Set $n = 0$ for pruning.
Else
  Set $n = 2n$ and update temporary support

$$G^{i+1} = \{j^i - 2n,\ j^i - n,\ j^i,\ j^i + n,\ j^i + 2n\}$$

End if
Apply off-grid OMP with the minimum spacing constraint
For $i = 1, 2, \ldots, J$ **do**
  Renew the partial-derivative matrix $\mathbf{P}_i$ and compute the pseudo-inverse

$$\mathbf{P}_i^+ = (\mathbf{P}_i^H \mathbf{P}_i)^{-1} \mathbf{P}_i^H$$

  Update the element position

$$x_k^{i+1} = \max\left\{ x_{k-1}^i + D,\ \min\left(x_{k+1}^i - D,\ x_k^i + \kappa x_k^i \Re([\mathbf{P}_i^+ \mathbf{r}_i^l]_k) \right) \right\}$$

  Reconstruct the steering matrix

$$\mathbf{\Phi}^{i+1} = [\mathbf{a}(x_1^{i+1}), \ldots, \mathbf{a}(x_t^{i+1})]$$

  Update the excitation coefficients

$$\mathbf{w}^{i+1} = \left((\mathbf{\Phi}_{i+1})^H \mathbf{\Phi}_{i+1} \right)^{-1} (\mathbf{\Phi}_{i+1})^H \mathbf{S}_d^l$$

End for
Until

$$\left\| \mathbf{S}_d^{(l)} - \sum_{k=1}^{t} w_k^{(l)}\, \mathbf{a}(x_k + \eta_k x_k) \right\|_2^2 \le \varepsilon$$

4. SIMULATION RESULTS AND ANALYSIS

To quantify the discrepancy between the reconstructed and desired radiation pattern, the normalized mean square error (NMSE) is employed as the matching error metric, which is defined as follows:

$$\text{NMSE} = \frac{\sum |S - S_d|^2}{\sum |S_d|^2} \tag{23}$$

In the simulation setup, a Chebyshev-weighted radiation pattern with a sidelobe level of -20 dB was selected as the optimization target. The array size was set to $M = 32$ with a spacing of 0.5λ. To verify the performance of the proposed algorithm in a multi-beam scanning scenario, the array was configured to steer the beams toward three representative spatial directions $[-10°, 0°, 10°]$, corresponding to three typical operating states.

First, simulation studies were conducted to evaluate the impact of the iteration number J on the overall synthesis performance of the proposed algorithm, and the results are illustrated in Fig. 1. In this study, the number of sparse elements was fixed at $t = 20$. As the iteration number increased, the NMSE exhibited an overall decreasing trend. When J reached approximately 6, a noticeable reduction in the NMSE was observed. For $J \ge 8$, the NMSE curve gradually converged, indicating that further increasing the number of iterations yielded only marginal performance improvements. Taking both radiation pattern reconstruction accuracy and computational complexity into account, the iteration number is set to $J = 10$ in the subsequent simulations. Fig. 2 shows the variation of NMSE with respect to the array sparsity level.

When the error threshold was set to $\varepsilon = 0.05$, Fig. 3 shows a comparison of the reconstructed radiation patterns obtained using the proposed algorithm and the desired patterns under three beam-scanning angles. The corresponding element position distributions and amplitude excitations of the designed sparse array are presented in Fig. 4. The results indicate that reconstructing the Chebyshev radiation patterns at the above three scanning angles requires $t = 24$ sparse elements. For the three scanning directions $[-10°, 0°, 10°]$, the matching errors between the reconstructed and desired radiation patterns were 0.01363, 0.00687, and 0.01363, respectively, demonstrating that the proposed algorithm can achieve accurate multi-beam pattern reconstruction under a relatively high sparsity level. Moreover, by incorporating a minimum spacing constraint of $D = 0.5\lambda$ into the algorithm, the resulting sparse array satisfies the condition that the distance between any two adjacent elements is no less than 0.5λ. This validates that the proposed method can maintain favorable pattern synthesis per-

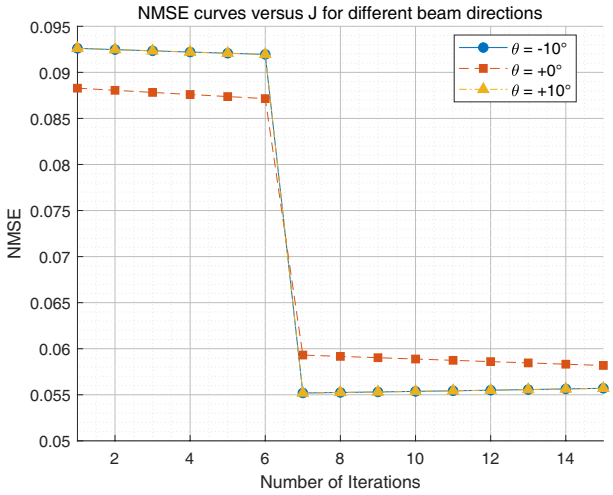

FIGURE 1. NMSE versus the iteration number J.

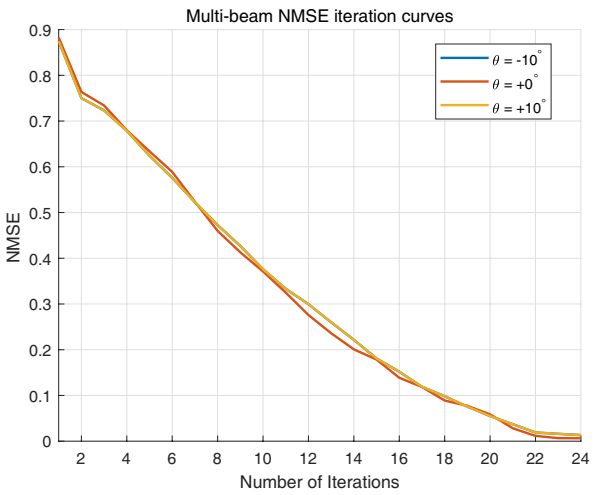

FIGURE 2. NMSE versus the array sparsity level t.

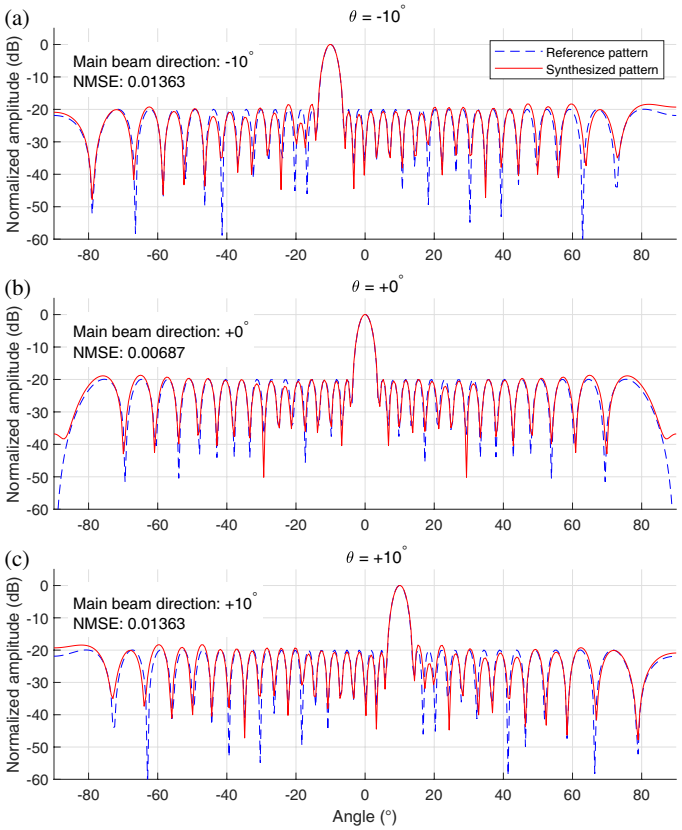

FIGURE 3. Comparison between the reconstructed radiation patterns obtained by the proposed algorithm and the desired patterns under three beam-scanning angles.

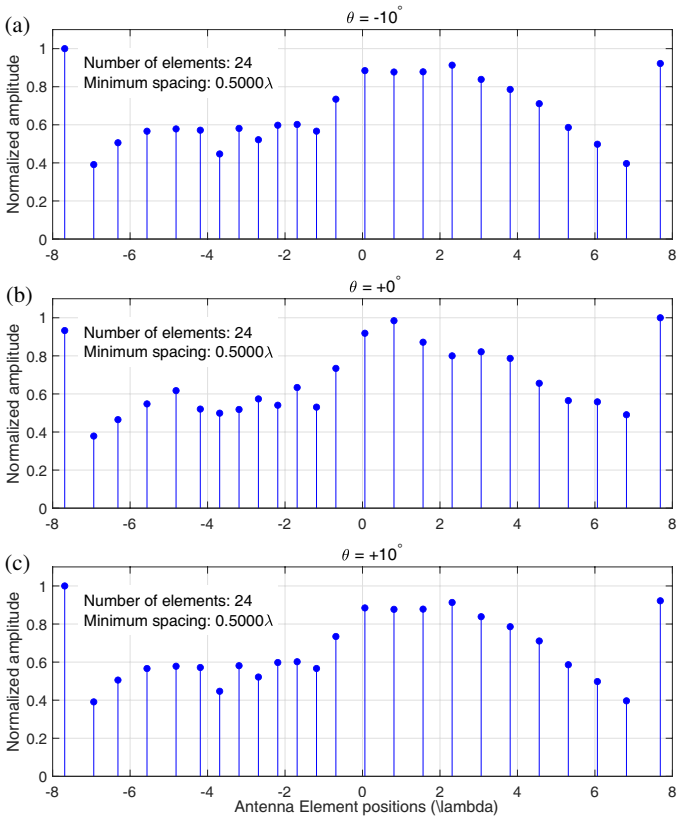

FIGURE 4. Element position distributions and amplitude excitations of the designed sparse array under three beam-scanning angles.

formance while complying with practical engineering implementation constraints.

To further evaluate the overall performance of the proposed G-OMP algorithm with a minimum spacing constraint, two benchmark methods were considered for comparison: the SAI-MFOCUSS algorithm and the MT-BCS algorithm, both subject to the same minimum spacing constraint. Fig. 5 shows the radiation pattern reconstruction results obtained by the SAI-MFOCUSS algorithm under a total array size of $M = 32$, where the number of elements after sparse reconstruction is $t = 21$, for three beam directions $[-10°, 0°, 10°]$. For these three scanning angles, the matching errors between the reconstructed and desired radiation patterns were 0.04511, 0.12531, and 0.04511, respectively. Fig. 6 shows the radiation pattern reconstruction results obtained by the MT-BCS algorithm under a total array size of $M = 32$, where the number of elements after sparse reconstruction is $t = 28$, for three beam directions

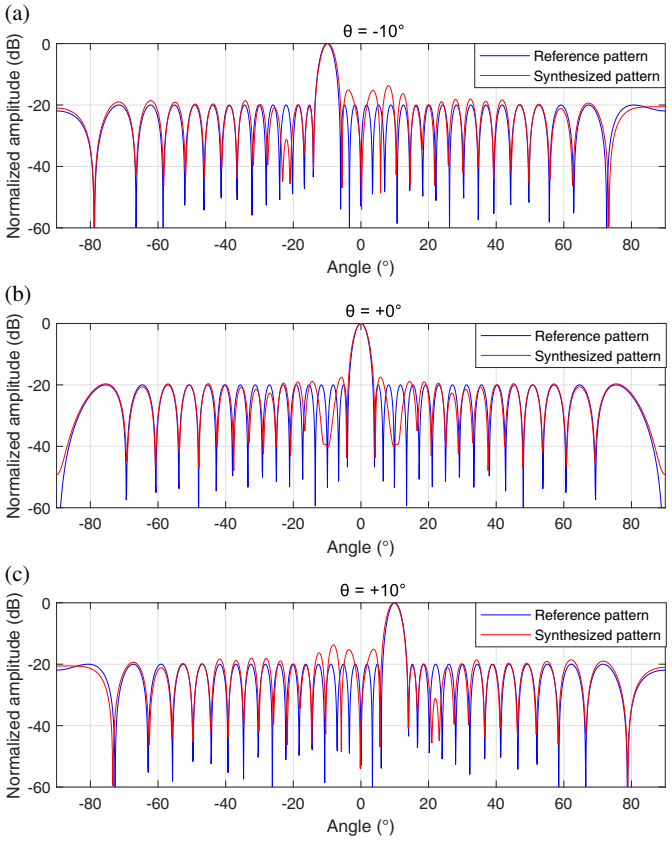

FIGURE 5. Radiation pattern reconstruction results obtained by the SAI-MFOCUSS algorithm under three beam-scanning angles.

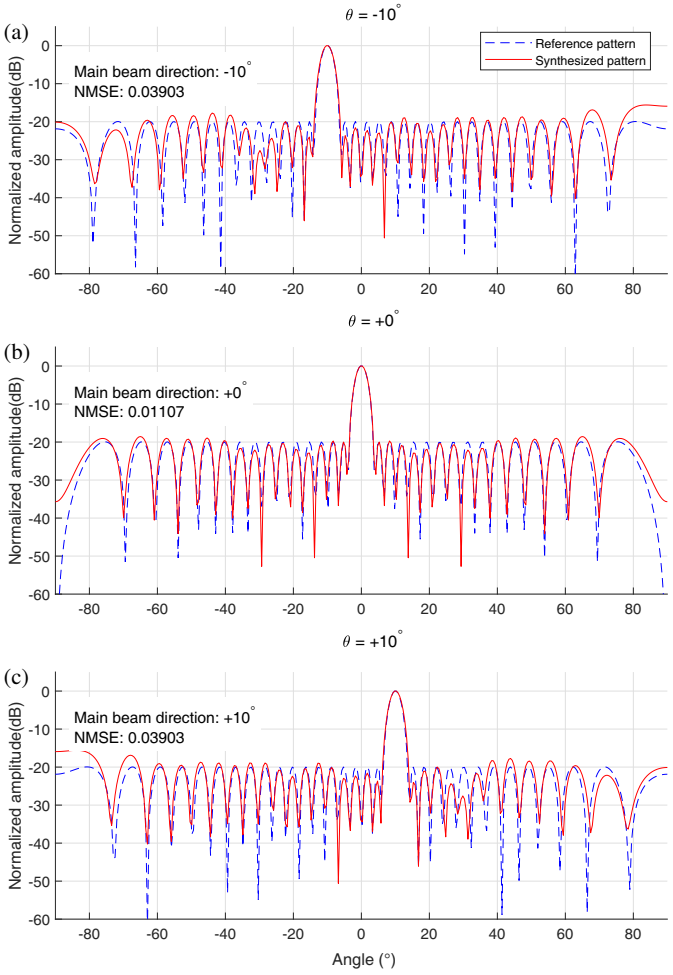

FIGURE 6. Radiation pattern reconstruction results obtained by the MTBCS algorithm under three beam-scanning angles.

$[-10°, 0°, 10°]$. For these three scanning angles, the matching errors between the reconstructed and desired radiation patterns were 0.03903, 0.01107, and 0.03903, respectively.

From the perspective of the optimization model, the MT-BCS algorithm introduces hierarchical sparse priors and iteratively updates the posterior distribution of the sparse coefficients. Under the same array apertures and minimum-spacing constraint, it generally requires a slightly larger number of array elements in sparse reconstruction. In addition, repeated posterior covariance updates are required during the solution process, and the dominant computational complexity increases approximately cubically with the grid size N. The SAI-MFOCUSS algorithm belongs to the class of non-convex sparsity-constrained reconstruction methods. It generally requires a slightly smaller number of array elements in sparse reconstruction, indicating that, under identical array apertures and minimum-spacing constraints, non-convex sparsification strategies exhibit certain advantages in terms of compressing the number of active elements. However, such non-convex optimization problems rely on iterative reweighting during the solution process, resulting in significantly higher computational complexities than convex optimization-based methods. In contrast, the proposed G-OMP algorithm with a minimum spacing constraint is based on a greedy selection strategy. In each iteration, it only involves correlation calculations and a limited number of least-squares problems. Consequently, its dominant computational complexity grows linearly with the dictionary size N and polynomially with the sparsity level t. Therefore, in large-scale multi-beam array application scenarios, the proposed method achieves favorable radiation pattern synthesis performance while incurring substantially lower computational complexities. Table 1 presents a comprehensive performance comparison among the three algorithms, where N_{out} and N_{in} denote the outer and inner iteration numbers of the SAI-MFOCUSS algorithm; J denotes the number of position-refinement iterations; N is the number of virtual array grid points; t represents the number of active elements selected in the sparse solution; P denotes the number of angle sampling points; T_{out} and I_{bcs} denote the outer iteration number and the internal evidence-maximization iteration number of the MT-BCS algorithm.

Finally, the computational efficiency of the three algorithms was evaluated by comparing the CPU runtimes required for the simulation experiments. All experiments were conducted on the same computing platform equipped with an Intel Core i5-10400F CPU @ 2.90 GHz and 32 GB RAM, using MATLAB R2022b. In addition, all three algorithms were tested under identical simulation settings. The above results show that the proposed G-OMP algorithm achieves the highest computational efficiency, which is also consistent with the preceding computational complexity analysis.

TABLE 1. Comprehensive performance comparison among the three algorithms.

Metric	Case	G-OMP	SAI-FOCUSS	MT-BCS
Number of Synthesized Elements	–	24	21	28
Computational Complexity	–	$O(PNt + JPt^3)$	$O\left(N_{out}\left[N_{in}(P^2N + P^3) + N^3\right]\right)$	$O(T_{out}I_{bcs}N^3) + O(T_{out}JPLt^2)$
CPU Runtime	–	2.14 s	3.58 s	27.47 s
NMSE	-10°	0.01363	0.04511	0.03903
	0°	0.00687	0.12531	0.01107
	10°	0.01363	0.04511	0.03903

5. CONCLUSION

This study proposes a low-complexity group-sparse orthogonal matching pursuit algorithm with a minimum spacing constraint. First, the sparse array synthesis problem is formulated based on compressive sensing theory. Subsequently, by incorporating group sparsity into the minimum-spacing-constrained off-grid OMP framework, a multi-beam reconfigurable radiation pattern is achieved. Finally, simulation results show that, in comparison with SAI-MFOCUSS and MT-BCS, the proposed algorithm achieves a good balance among radiation pattern performance, element sparsity, and computational complexity.

It should be noted that the proposed method is still essentially a greedy algorithm. Therefore, its solution quality may be affected by the local optimality nature of greedy pursuit, and the obtained result is not guaranteed to be globally optimal. In addition, the mutual coupling effect is treated in a simplified manner in the current study, which may not fully reflect more complicated practical array environments. These issues will be further investigated in future work by considering more robust optimization strategies and more realistic mutual coupling models.

REFERENCES

[1] Van Trees, H. L., *Optimum Array Processing: Part IV of Detection, Estimation, and Modulation Theory*, John Wiley & Sons, 2002.

[2] Eisenbeis, J., T. Mahler, P. R. Lopez, and T. Zwick, "Channel estimation method for subarray based hybrid beamforming systems employing sparse arrays," *Progress In Electromagnetics Research C*, Vol. 87, 25–38, 2018.

[3] Tang, Q., B. Wang, and X. Tian, "Synthesis of antenna array based on hybrid improved sparrow search algorithm and convex programming," *Progress In Electromagnetics Research C*, Vol. 153, 247–255, 2025.

[4] Zhao, X. and Y. Zhang, "An off-grid compressed sensing method for synthesis of maximally sparse arrays with arbitrary beampatterns," *Progress In Electromagnetics Research C*, Vol. 126, 227–241, 2022.

[5] Wang, L., X.-K. Wang, G. Wang, and J.-K. Jia, "A two-step method for the low-sidelobe synthesis of uniform amplitude planar sparse arrays," *Progress In Electromagnetics Research M*, Vol. 86, 153–162, 2019.

[6] Battaglia, G. M., A. F. Morabito, G. Sorbello, and T. Isernia, "Mask-constrained power synthesis of large and arbitrary arraysas a few-samples global optimization," *Progress In Electromagnetics Research C*, Vol. 98, 69–81, 2020.

[7] Ullah, N., Z. Huiling, T. Rahim, S. U. Rahman, and M. MuhammadKamal, "Reduced side lobe level of sparse linear antenna array by optimized spacing and excitation amplitude using particle swarm optimization," in *2017 7th IEEE International Symposium on Microwave, Antenna, Propagation, and EMC Technologies (MAPE)*, 96–99, Xi'an, China, 2017.

[8] Chen, K., X. Yun, Z. He, and C. Han, "Synthesis of sparse planar arrays using modified real genetic algorithm," *IEEE Transactions on Antennas and Propagation*, Vol. 55, No. 4, 1067–1073, 2007.

[9] Wang, X. P., P. F. Gu, D. Z. Ding, and R. S. Chen, "Unitary matrix pencil method for multi-beam sparse linear array pattern synthesis," in *2017 International Applied Computational Electromagnetics Society Symposium (ACES)*, 1–2, Suzhou, China, 2017.

[10] Candes, E. J. and M. B. Wakin, "An introduction to compressive sampling," *IEEE Signal Processing Magazine*, Vol. 25, No. 2, 21–30, 2008.

[11] Oliveri, G. and A. Massa, "Bayesian compressive sampling for pattern synthesis with maximally sparse non-uniform linear arrays," *IEEE Transactions on Antennas and Propagation*, Vol. 59, No. 2, 467–481, Feb. 2011.

[12] Zhou, W., M. Shen, D. Wu, and D. Zhu, "Efficient beam-scanning wideband sparse array synthesis with minimum element spacing control," *Signal Processing*, Vol. 238, 110194, 2026.

[13] Wang, Z., M. Xu, M. Shen, and Y. Shen, "Pattern-reconfigurable sparse array synthesis with minimum element spacing constraint," *Journal of Electromagnetic Waves and Applications*, Vol. 39, No. 7, 810–821, 2025.

[14] Yang, Z., L. Xie, and C. Zhang, "Off-grid direction of arrival estimation using sparse bayesian inference," *IEEE Transactions on Signal Processing*, Vol. 61, No. 1, 38–43, Jan. 2013.